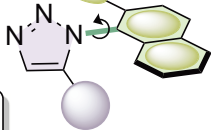
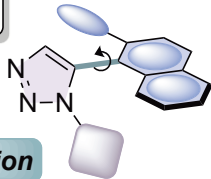


**C-N Restricted Rotation**

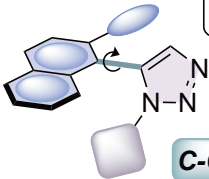
*Most stable*



**1,2,3-Triazoles  
1,5-Di-substituted  
Atropisomers  
Axial chirality**



**C-C Restricted Rotation**



# Enantiomer stability of atropisomeric 1,5-disubstituted 1,2,3-triazoles

Fernanda Meloni,<sup>(a)</sup> William D. G. Brittain,<sup>(a,b)</sup> Louise Male,<sup>(c)</sup> Cécile S. Le Duff,<sup>(d)</sup>  
Benjamin R. Buckley,<sup>\*(e)</sup> Andrew G. Leach, <sup>\*(f)</sup> and John S. Fossey <sup>\*(a)</sup>

<sup>(a)</sup> School of Chemistry, University of Birmingham, Edgbaston, Birmingham, West Midlands, B15 2TT, U.K.

<sup>(b)</sup> Present Address: Department of Chemistry, Durham University, Durham, DH1 3LE, U.K. <sup>(c)</sup> X-Ray Crystallography Suite, School of Chemistry, University of Birmingham, Edgbaston, Birmingham, West Midlands, B15 2TT, U.K. <sup>(d)</sup> NMR Spectroscopy Suite, School of Chemistry, University of Birmingham, Edgbaston, Birmingham, West Midlands, B15 2TT, U.K. <sup>(e)</sup> Department of Chemistry, Loughborough University, Loughborough, Leicestershire, LE11 3TU, U.K. <sup>(f)</sup> School of Health Sciences, Stopford Building, The University of Manchester, Oxford Road, Manchester M13 9PT, U.K.

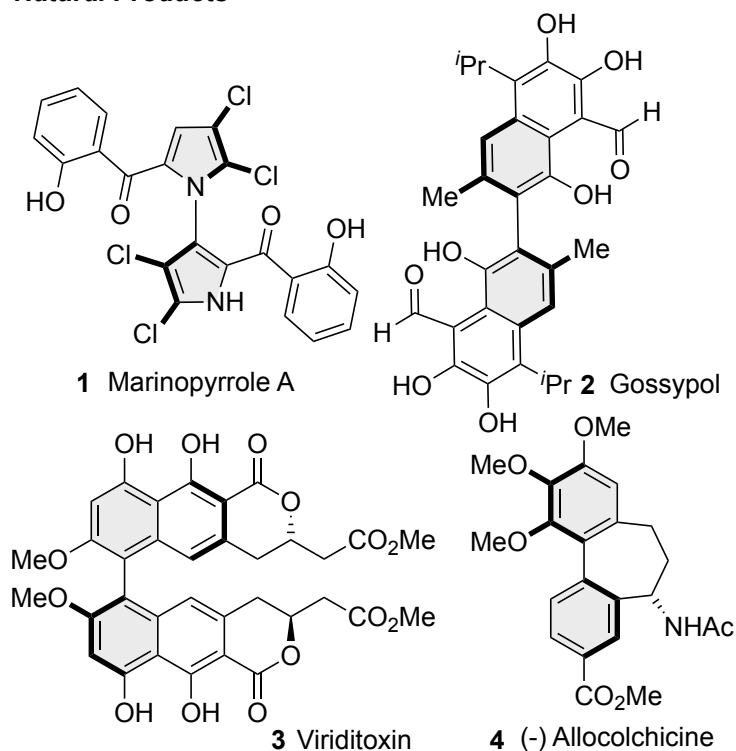
## Abstract

The synthesis and characterisation of axially chiral atropisomeric 1,5-disubstituted 1,2,3-triazoles is reported. Molecules designed to display restricted rotation about 1,2,3-triazole *N*-1-aryl or 1,2,3-triazole *C*-5-aryl bonds were investigated by physical and computational techniques. The barrier to 1,2,3-triazole *N*-1-aryl rotation was found to be higher than that for 1,2,3-triazole *C*-5-aryl rotation, confirming axial chirality stemming from restricted rotation about an *N*-1-aryl bond in a 1,5-disubstituted 1,2,3-triazole to be the most suitable for the development of an axial chirality triazole-based platform.

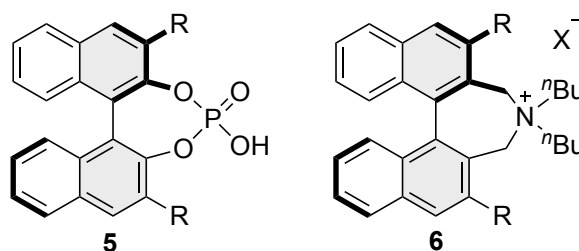
## Introduction

Compounds that are chiral by virtue of restricted single bond rotation are among those said to display axial chirality.<sup>1-3</sup> The stability of these atropisomers (from the Greek prefix *atrops*, “not turning”)<sup>4</sup> is determined by the magnitude of the rotational barrier  $\Delta G^\ddagger$ . The barrier to rotation can be influenced by factors such as the degree of steric hindrance, inter- and intramolecular interactions, temperature and the solvent.<sup>5</sup> A generally accepted definition of an atropisomer is a compound where the single bond whose rotamers are stereoisomers of each other and the half-life for their interconversion is at least 1000 s (16.7 min), at a given temperature. In principle, this allows sufficient time to carry out a routine physical separation of the enantiomeric rotamers (i.e. atropisomers), thus implying, at room temperature,  $\Delta G^\ddagger$  should be at more than about 22 kcal·mol<sup>-1</sup> for the interconversion of these stereoisomers by, overall, single bond rotation to impart functional and physically manageable axial chirality upon the system.<sup>6</sup>

### Natural Products



### Organocatalysts



### Ligands

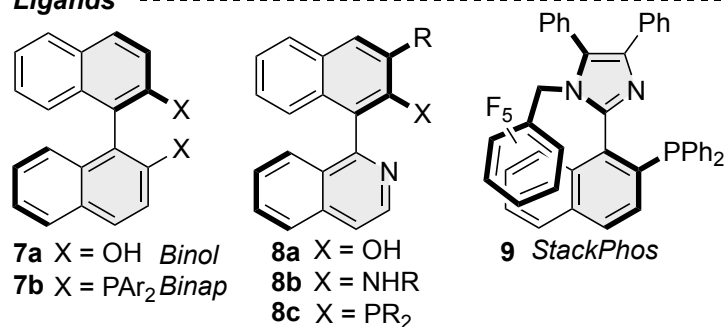


**Figure 1.** Selected examples of atropisomeric compounds. Upper: Natural products Marinopyrrole A (**1**); Gossypol (**2**); Viridotoxin (**3**); (-)-Allocolchicine (**4**). Middle: Organocatalysts chiral phosphoric acid derivatives (**5**); chiral ammonium salts (**6**). Lower: Chiral ligands BINOL (**7a**) and BINAP (**7b**); QUINAP derivatives (**8a-c**); StackPhos (**9**).

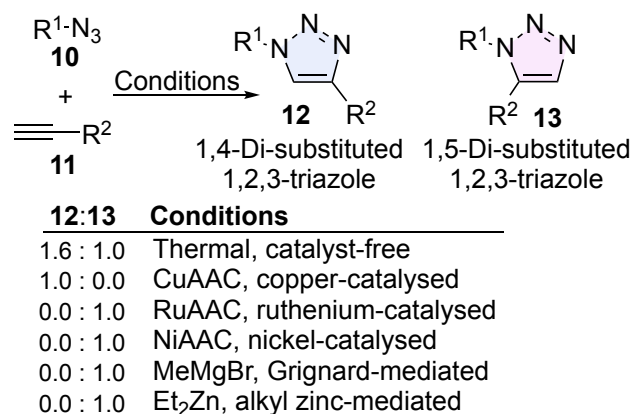
Many natural products exhibit axial chirality,<sup>7</sup> for example marinopyrrole A (**1**),<sup>8</sup> gossypol (**2**),<sup>9</sup> viridotoxin (**3**)<sup>10</sup> and allocolchicine (**4**)<sup>11</sup> contain a single bond between two sp<sup>2</sup> atoms whose restricted rotation and non-zero dihedral angle between substituents in a stable conformation confers axial chirality upon them (Figure 1). Axially chiral compounds are finding ever more utility in stereoselective synthesis, particularly as chirality platforms in drug discovery<sup>12-16</sup> and asymmetric catalysis. Organocatalysts, such as chiral phosphoric acid derivatives **5**<sup>17</sup> chiral

ammonium salts **6**<sup>18, 19</sup> and chiral ligands including BINOL,<sup>20, 21</sup> BINAP,<sup>22</sup> QUINAP<sup>23</sup> and StackPhos,<sup>24, 25</sup> all exploit restricted rotation about a single bond between two sp<sup>2</sup> atoms to engender asymmetry and thus impart further asymmetry in the products of the reactions they have been reported to catalyse. In contrast to well-reported examples of chirality arising because of restricted rotation between two six-membered rings, atropisomerically pure axially chiral compounds with the chirality-conferring restricted bond rotation being to or between five-membered rings are relatively under-reported.<sup>26-32</sup>

The 1,2,3-triazole represents a five-membered heterocycle that has seen increasing interest in a variety of applications. Disubstituted 1,2,3-triazoles are most frequently reported as 1,4-disubstituted 1,2,3-triazoles (**12**) and somewhat less frequently as regio-isomeric 1,5-disubstituted 1,2,3-triazoles (**13**). Such triazoles have found wide-ranging application beyond serving as linking motifs, displaying intra- and intermolecular interactions resulting in a myriad of functional and scaffolding applications in supramolecular,<sup>23-34</sup> coordination,<sup>35-37</sup> medicinal,<sup>38, 39</sup> drug discovery,<sup>40</sup> sensor<sup>41, 42</sup> and catalytic<sup>43-50</sup> chemistries. These triazoles are stable at elevated temperatures and under biological conditions rendering them amenable to development for applications in materials<sup>51, 52</sup> and chemical biology.<sup>53</sup>

The synthesis of 1,2,3-triazoles was first reported under thermal conditions *via* the (since-named) *Huisgen 1,3-dipolar cycloaddition* between azides and alkynes to access mixtures of 1,4-disubstituted 1,2,3 triazoles (**12**) and 1,5-disubstituted 1,2,3-triazoles (**13**).<sup>54, 55</sup> The low regiochemical control (1.6:1.0 ratio of **12:13**) of this reaction,<sup>56</sup> led to the search for catalysts to promote variants of the dipolar cycloaddition between alkynes and azides. The most successful variant was reported in 2002 by both Sharpless and co-workers<sup>56</sup> and Meldal and co-workers,<sup>57</sup> where copper-catalysed 1,2,3-triazole formation was achieved under mild conditions. The copper-catalysed azide-alkyne cycloaddition (CuAAC) has become the most well-known and utilised protocol for accessing 1,4-disubstituted 1,2,3-triazoles (**12**). Despite being one of a number of *click reactions* the CuAAC is often referred to as “*the click reaction*” after it was included in Sharpless and co-workers’ seminal introduction of “*click chemistry*” as a concept.<sup>58, 59</sup> The CuAAC is widely utilised as a universal linking strategy, it can be carried out at room temperature in benign solvents and is compatible with *in vivo* use, giving exquisite regiochemical control in the 1,4-disubstituted triazole products (1:0 **12:13**, Scheme 1). Whilst the CuAAC provides unparalleled facile access to 1,4-disubstituted 1,2,3-triazoles, 1,5-disubstituted analogues are less-frequently reported. Among the protocols available for the synthesis of 1,5-disubstituted triazole derivatives are the *in situ* generation of metallo-alkyne reagents by treatment of a terminal alkyne (**11**) with organo-magnesium<sup>60</sup> (Grignard) and

organo-zinc<sup>61</sup> reagents, which upon reaction with an azide (**10**) form exclusively 1,5-disubstituted-1,2,3-triazoles (0.0:1.0 **12:13**). Ruthenium- and nickel- catalysed azide-alkyne cycloaddition reactions, RuAAC<sup>62-64</sup> and NiAAC<sup>46, 65</sup> respectively (Scheme 1) also offer access to 1,5-disubstituted 1,2,3-triazoles.



**Scheme 1.** 1,2,3-Triazole-forming azide (**10**) - alkyne (**11**) cycloaddition reactions giving mixtures of 1,4- and 1,5-disubstituted products (**12** and **13** respectively) under metal-free (thermal) conditions, in contrast to the exclusive formation of the 1,4-disubstituted isomer (**12**) under copper-catalysed conditions or highly selective formation of the 1,5- isomer (**13**) under control of ruthenium or nickel catalysis or magnesium or zinc stoichiometric promoters.

Despite the prevalence of reports of 1,2,3-triazoles it is somewhat surprising that examples of well-characterised axially chiral atropisomeric compounds featuring a rotationally restricted, non-zero dihedral angle, bond to or from 1,2,3-triazoles are scarce and, despite two notable examples (**14**)<sup>66</sup> and (**15**),<sup>67</sup> they are mostly limited to 5-5'-bistriazoles (**16** and **17**) (Figure 2).<sup>30, 68-70</sup> Notably their chirality is conferred by restricted rotation about a bond with C5 of the 1,4,5-trisubstituted 1,2,3-triazole(s) in question.

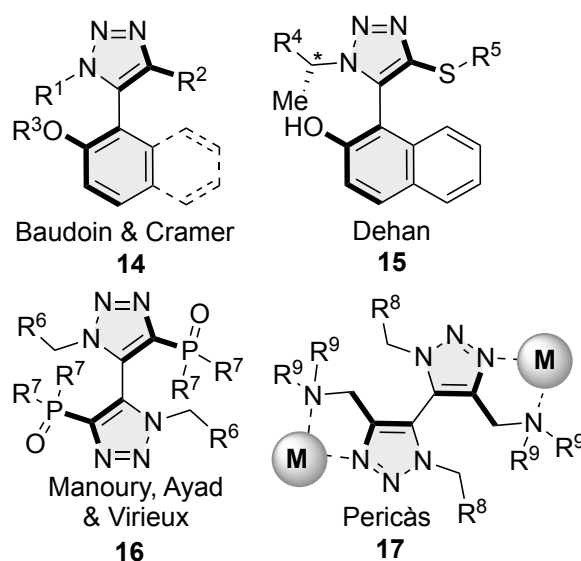


**Figure 2.** Previously reported chiral atropisomeric 1,4,5-trisubstituted 1,2,3-triazoles **14-17** whereby the restricted bond conferring chirality is a C-C bond to the 5-position of said 1,2,3-triazole.<sup>30, 66-70</sup>

Authors of this report have previously investigated and surveyed 1,2,3-triazoles as scaffolds for sensor assembly,<sup>71-74</sup> as ligand platforms,<sup>75, 76</sup> in asymmetric synthesis<sup>77-79</sup> and as linkers,<sup>80, 81</sup> and in this report axial chirality of atropisomeric 1,5-substituted 1,2,3-triazoles is probed.

## Results and Discussion

In order to probe axial chirality through restricted bond rotation at the 1- or 5- positions of 1,5-disubstituted 1,2,3-triazoles, appropriate functional groups were contemplated. Such compounds should be sterically congested, synthetically accessible and offer spectroscopic handles by which to probe asymmetry.

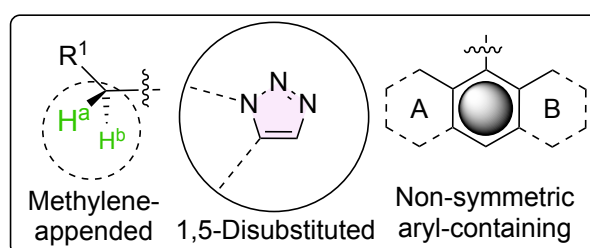
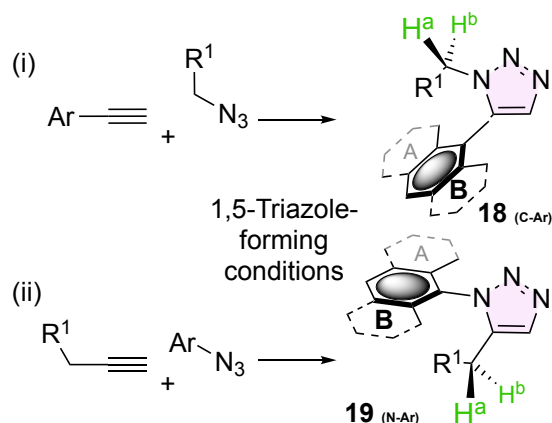


**Figure 3.** Hypothesised features of 1,5-disubstituted 1,2,3-triazoles that may display axial chirality about an  $sp^2$ - $sp^2$  bond from either N-1 or C-5 of the triazole to a non-symmetric aryl group. The hypothesised compound includes potentially diastereotopic functionality (arbitrarily depicted as a methylene group  $CH^aH^b$ ).

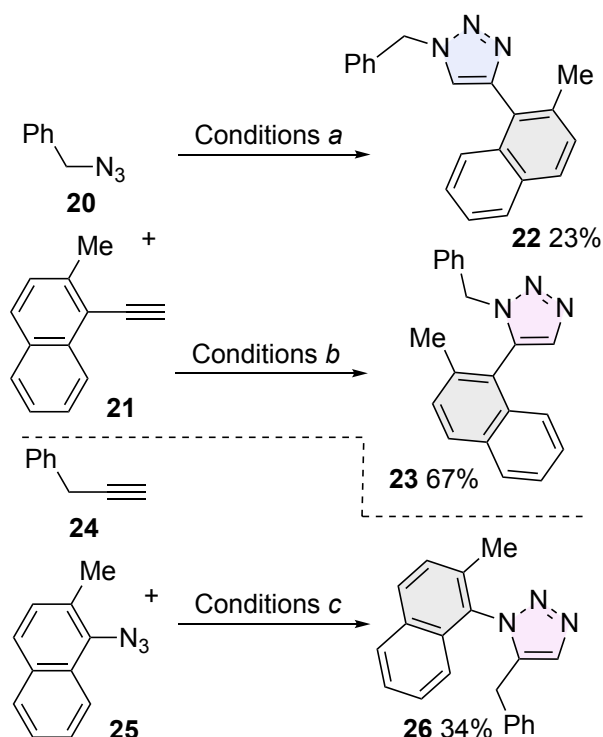
At least one functional group should be bound to the triazole *via* an  $sp^2$  atom and that  $sp^2$  atom must be dissymmetrically substituted (such that restricted rotation leads to the formation of non-planar, chiral products). The second substituent at the remaining 1- or 5- position of the 1,2,3-triazole ought to be both bulky enough to offer steric constraints to rotation of its  $sp^2$ - $sp^2$  conjoined neighbour and include diastereotopic functionality (e.g a  $CH_2$  methylene group) as a NMR spectroscopic handle (Figure 3). NMR-active nuclei-containing diastereotopic groups offer two opportunities to probe any resulting axially chiral materials: (i) observation of two distinct signals for the groups (e.g. the protons of a  $CH_2$  group) provides compelling evidence that the molecule is chiral with rotation perturbed to such an extent that their difference is witnessable on the NMR-timescale; (ii) temperature- (and other condition-) dependence of the observation of one *versus* two signals (with emergence of any evidence of the environments not being equivalent) may corroborate the lack or presence of chirality and/or rapid (racemisation) and slow (stable axial chirality) rotation about the  $sp^2$ - $sp^2$  bond in question. Two series of 1,5-disubstituted 1,2,3-triazoles were initially proposed (Scheme 2): (i) a corresponding triazole is formed from an appropriate aryl-alkyne and a methylene-appended azide, resulting in a 1,5-disubstituted product with a potentially restricted  $C(sp^2)$ - $C(sp^2)$  bond at the C-5 position and a methylene-bearing group with potentially diastereotopic protons therein appended to the N-1 position **18** (<sub>(C-Ar)</sub>); and (ii) the isomeric 1,5-disubstituted product

whereby a methylene-appended alkyne and an appropriate aryl-azide are reacted under 1,5-triazole-forming conditions to furnish a product with a potentially rotation-restricted chirality-conferring N(sp<sup>2</sup>)-C(sp<sup>2</sup>) bond appended to N-1 of the triazole and potentially diastereotopic protons appended to the C-5 position **19** (N-Ar).



**Scheme 2.** Proposed syntheses of 1,5-disubstituted 1,2,3-triazoles with: (i) a C-C restricted-rotation bond and a CH<sub>2</sub> group attached to N-1 (**18** (C-Ar)); and (ii) a C-N restricted-rotation bond and a CH<sub>2</sub> group attached to C-5 (**19** (N-Ar)).

Benzyl and 2-methyl-1-substituted naphthalene were initially selected as functional groups offering desired features potentially capable of conferring and reporting on chirality of corresponding 1,5-disubstituted 1,2,3-triazoles. Starting with benzyl azide **20** and 1-ethynyl-2-methylnaphthalene **21** both the 1,4-(control) and 1,5-(probe) disubstituted triazoles **22** (23% yield) and **23** (67% yield) were prepared by a CuAAC and by treatment with methylmagnesium bromide respectively (Scheme 3, upper and middle respectively). Since 1,4-disubstituted **22** does not feature contiguous substitution about the triazole core, no rotation-restriction is expected at room temperature, and it therefore serves as an achiral control. Whilst 1,5-disubstituted **23** was successfully prepared by stoichiometric addition of organomagnesium compounds it is noteworthy, that in our hands, a ruthenium-catalysed alkyne-azide cycloaddition (RuAAC)<sup>64</sup> protocol gave only trace amounts of the desired product. It had been noted by Mahadari *et al.* that sterically demanding substrates tend to under-perform in RuAAC reactions where bulky substituents are desired about 1,5-disubstituted 1,2,3-triazoles.<sup>82</sup> A RuAAC approach was suspended in favour of the higher-yielding magnesium-mediated method that successfully delivered **23**. Prop-2-yn-1-ylbenzene **24** and 1-azido-2-methylnaphthalene **25** were reacted *via* a diethyl zinc protocol to give regioisomeric product **26** in 34% isolated yield (Scheme 3, lower).



**Scheme 3.** Upper: Reaction of **20** and **21** under conditions (a) Copper sulfate pentahydrate (20 mol%), sodium ascorbate (20 mol%), DMF, MW 150 °C, 30 min resulting in isolation of **22** in 23% isolated yield; middle: Reaction of **20** and **21** under conditions (b) Methylmagnesium bromide (3.0 M in hexane), THF resulting in isolation of **23** in 67% isolated yield; lower: Reaction of **24** and **25** under conditions (c) Diethyl zinc (1.0 M in hexane), NMI (20 mol%), THF resulting in isolation of **26** in 34% isolated yield.

Inspection of the methylene region of the proton NMR spectra of (i) **22**; (ii) **23** and (iii) **26** in chloroform- $D$  at room temperature (Figure 4, left, middle and right respectively), shows (i) a singlet with an integration corresponding to two protons (protons labelled  $H^a$  and  $H^b$ ), consistent with **22** being an overall achiral molecule; (ii) and (iii) (**23** and **26**, respectively) both revealed a pair of one-proton doublets in each spectrum, displaying  $^2J$  coupling values diagnostic of the methylene group's protons (labelled  $H^a$  and  $H^b$ ) both being rendered diastereotopic as a result of being in a chiral environment. Thus, 1,4-disubstituted **22** does not display functional axial chirality whilst both 1,5-regio isomers **23** and **26** are axially chiral, on the NMR timescale.<sup>83</sup>

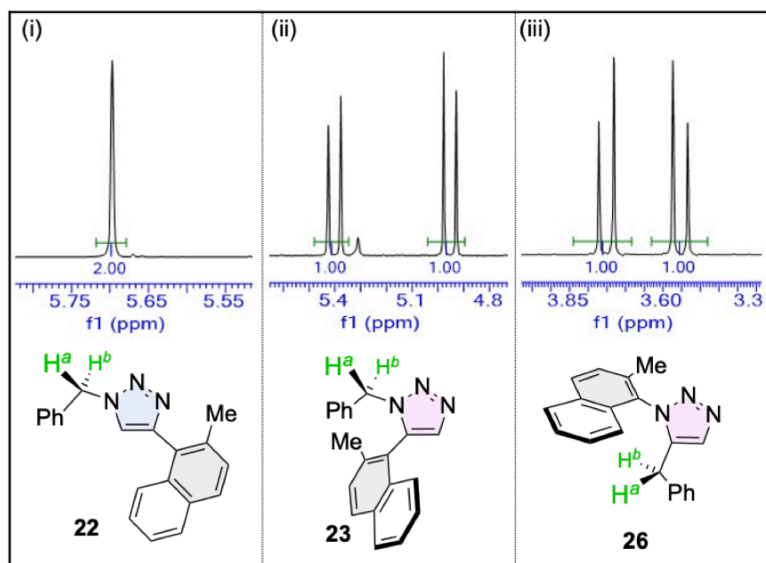


**Figure 4.** Regions of the proton NMR spectrums of **22**, **23** and **26**, recorded in  $CDCl_3$  at room temperature; (i) a single resonance arising from equivalent methylene protons  $H^a$  and  $H^b$  in achiral **22**; (ii) two doublets corresponding to diastereotopic methylene protons  $H^a$  and  $H^b$  in chiral **23**; and (iii) two doublets corresponding to diastereotopic methylene protons  $H^a$  and  $H^b$  in chiral **26**.

It was reasoned that recording a proton NMR spectrum at elevated temperature may lead to coalescence of diastereotopic signals, through which a barrier to enantiomer interconversion could be determined. As such compound **23** was subjected to proton NMR analysis in tetrachloroethane- $d_2$  (TCE) at elevated temperatures in 10 °C steps from 20 to 100 °C. Pleasingly for this study the benzylic methylene protons  $H^a$  and  $H^b$  did not coalesce over this range. Changing the solvent to toluene- $d_8$  elicited no significant changes, suggesting that the barrier to rotation of **23** in deuterated TCE or toluene is at least 24 kcal·mol $^{-1}$  (see supplementary details for stacked plots).

Regioisomeric, axially chiral, 1,5-disubstituted 1,2,3-triazoles **23** and **26** could be resolved by analytical HPLC on a chiral stationary phase (Lux Phenomenex Cellulose-1, water/acetonitrile, Figure 5 (i) and (ii) respectively). In both cases, the lack of an obvious plateau between adjacent peaks corresponding to enantiomers (*i.e.* “batman peak” indicative of on-column enantiomer interconversion)<sup>84</sup> is consistent with atropisomeric stability.

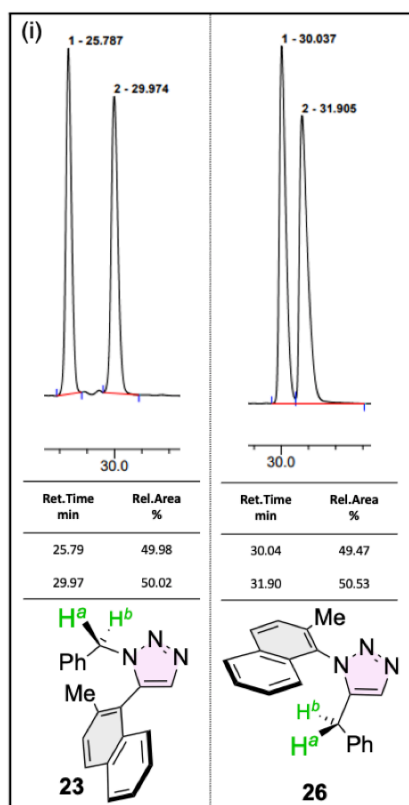


**Figure 5.** HPLC chromatograms of racemic triazoles using a chiral stationary phase: (i) **23** and (ii) **26**; 50:50 (v/v) water/acetonitrile, 1 mL.min<sup>-1</sup>; Lux Phenomenex Cellulose-1.

Scalemic samples of **23** and **26** were obtained by preparative HPLC using a chiral stationary phase (95 and 60% e.e. respectively). These samples were used to experimentally determine barriers to rotation about the triazole-aryl bond conferring axial chirality upon them (enantiomer interconversion), by HPLC analysis. Samples were hence dissolved in acetonitrile and the resulting solutions heated at 70 °C for eight hours, under which conditions analytical HPLC analysis revealed enantiopurity of C-C axially chiral **23** was eroded, whereas the enantiopurity of N-C axially chiral **26** was essentially unchanged. To witness a significant reduction in the e.e. of **26** an acetonitrile solution of scalemic material needed to be heated at 80 °C for more than 100 hours. As such, aliquots of acetonitrile solutions of **23** or **26** (that were being heated at 70 or 80 °C respectively) were collected at regular intervals and the e.e. of the solutions measured by chiral HPLC analysis (Figure 6). Deploying the Eyring equation allowed respective barriers to rotation (enantiomer interconversion) to be assessed as 25.0 kcal.mol<sup>-1</sup> and 29.0 kcal.mol<sup>-1</sup> for (C-C axially chiral) **23** and (C-N axially chiral) **26** respectively. Assuming that  $\Delta S^\ddagger$  for bond rotations is expected to be small,<sup>85</sup>  $\Delta G^\ddagger$  is expected to vary little with temperature, so that, on a first approximation, the  $\Delta G^\ddagger$  obtained can be compared to computed values discussed later.

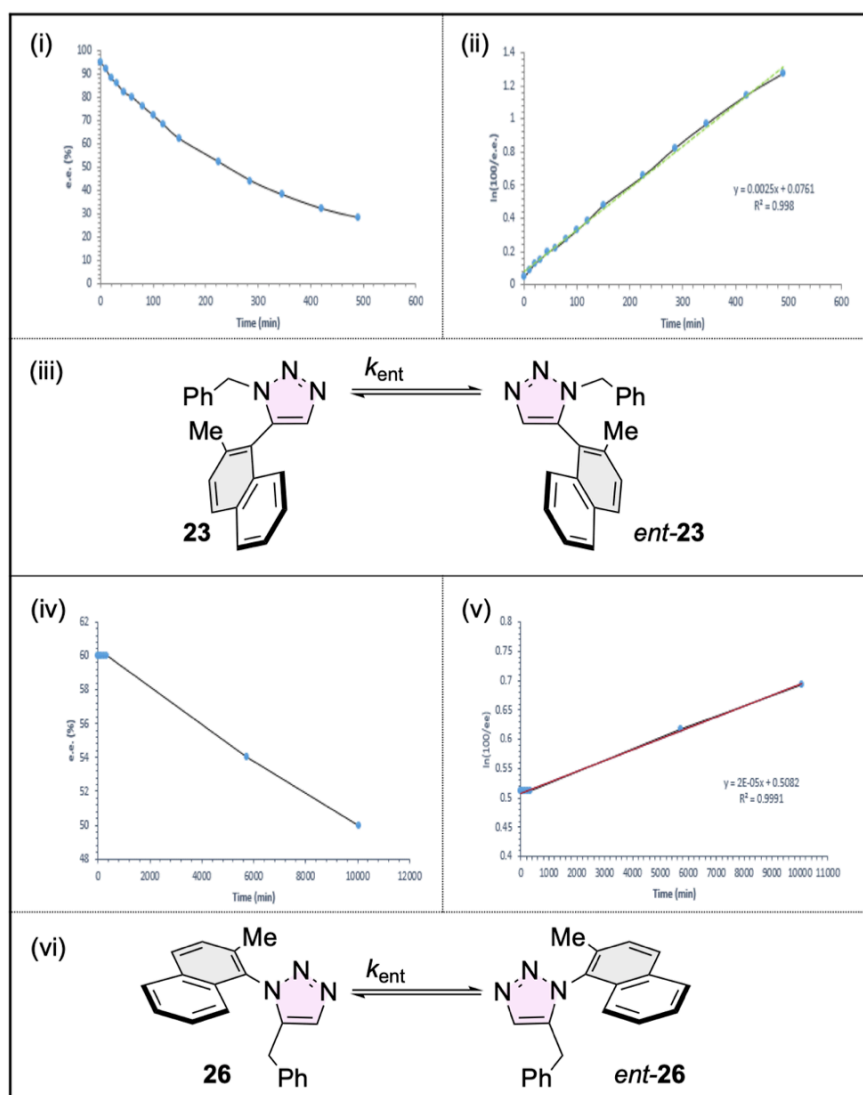


**Figure 6.** (i) e.e.% decay of **23** over time ; (ii)  $\ln(100/e.e.)$  over time in **23**; (iii) Enantiomerisation of **23**; (iv) e.e.% decay of **26** over time; (v)  $\ln(100/e.e.)$  over time in **26**; (vi) Enantiomerisation of **26**.

To explore these barriers in more detail and to establish the structural features that increase and decrease the barriers, density functional theory calculations were performed. Initial calculations employed the restricted Hartree-Fock (RHF) method combined with dihedral rotational scans to provide connection to earlier studies,<sup>86</sup> and these also yielded geometries that were subsequently optimised with M06-2X/6-31+G\*, permitting the computation of free energy barriers that could be compared with those measured. This level of theory was designed to provide good agreement with barrier heights.<sup>87, 88</sup> Solvation was included *via* the integral equation formalism polarisable continuum model (IEFPCM) protocol and included parameters appropriate to acetonitrile.<sup>89</sup> All calculations were performed in Gaussian09.<sup>90</sup> In the studies of C-C axially chiral **23** (Figure 7, upper panel), it was found that there are two alternative transition states for rotation; the one in which the benzyl group passes the methyl group is the lowest energy (a dihedral N-C-C-C angle<sup>91</sup> about the bond conferring axially chirality of +172.6°

[akin to a pseudo planar  $+180^\circ$  dihedral angle]), and is calculated to represent a free energy barrier of  $30.0 \text{ kcal}\cdot\text{mol}^{-1}$ . The transition state to enantiomer interconversion, by single bond rotation, where the benzyl group passes the peri-CH of the naphthalene ring (dihedral N-C-C-C angle about the bond conferring axially chirality  $-15.2^\circ$  [analogous to pseudo planar  $0^\circ$  dihedral angle]) is  $2.8 \text{ kcal}\cdot\text{mol}^{-1}$  higher in energy. In equivalent studies of **26** (Figure 7, lower panel), the preference is reversed, and the barriers are higher. The transition state that sees the benzyl group passing the peri-CH (a dihedral N-N-C-C angle about the bond conferring axially chirality of  $+199.7^\circ$  [similar to a pseudo planar  $+180^\circ$  dihedral angle]) corresponds to a free energy barrier of  $33.2 \text{ kcal}\cdot\text{mol}^{-1}$ , while that in which it passes the methyl group (a dihedral N-N-C-C angle about the bond conferring axially chirality of  $+7.7^\circ$  [comparable to a pseudo planar  $0^\circ$  dihedral angle]) is at  $35.2 \text{ kcal}\cdot\text{mol}^{-1}$ .

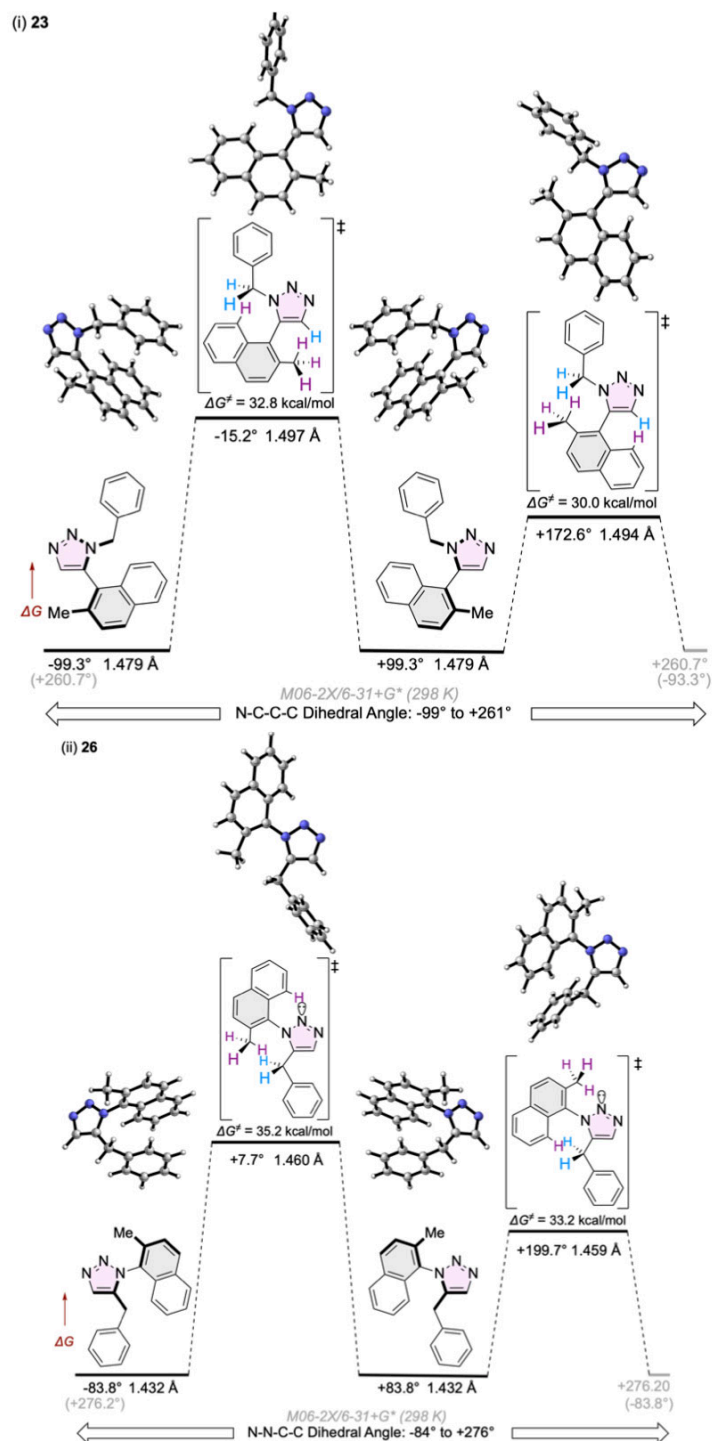


**Figure 7.** Energy level diagrams for the rotation about the chiral axis in: (i) **23** (upper) and; (ii) **26** (lower). 3D representations of the computed maxima and minima are shown. Calculations are at the M06-2X/6-31+G\* level of theory including solvation via the IEFPCM model and were performed in Gaussian09.<sup>90</sup> Free energies at 298 K are computed using GoodVibes.<sup>92</sup>

Both the experimentally and computationally determined barriers to atropisomer interconversion concur that axial chirality about the triazole-aryl C-C bond in **23** (25.0 and 30.0 kcal·mol<sup>-1</sup> respectively) is less stable than in regioisomeric triazole-aryl N-C **26** (29.0 and 33.2 kcal·mol<sup>-1</sup> respectively). This implies that N-C triazole-aryl axial chirality is inherently more stable to enantiomer interconversion than regioisomeric C-C triazole aryl bonds. However, the

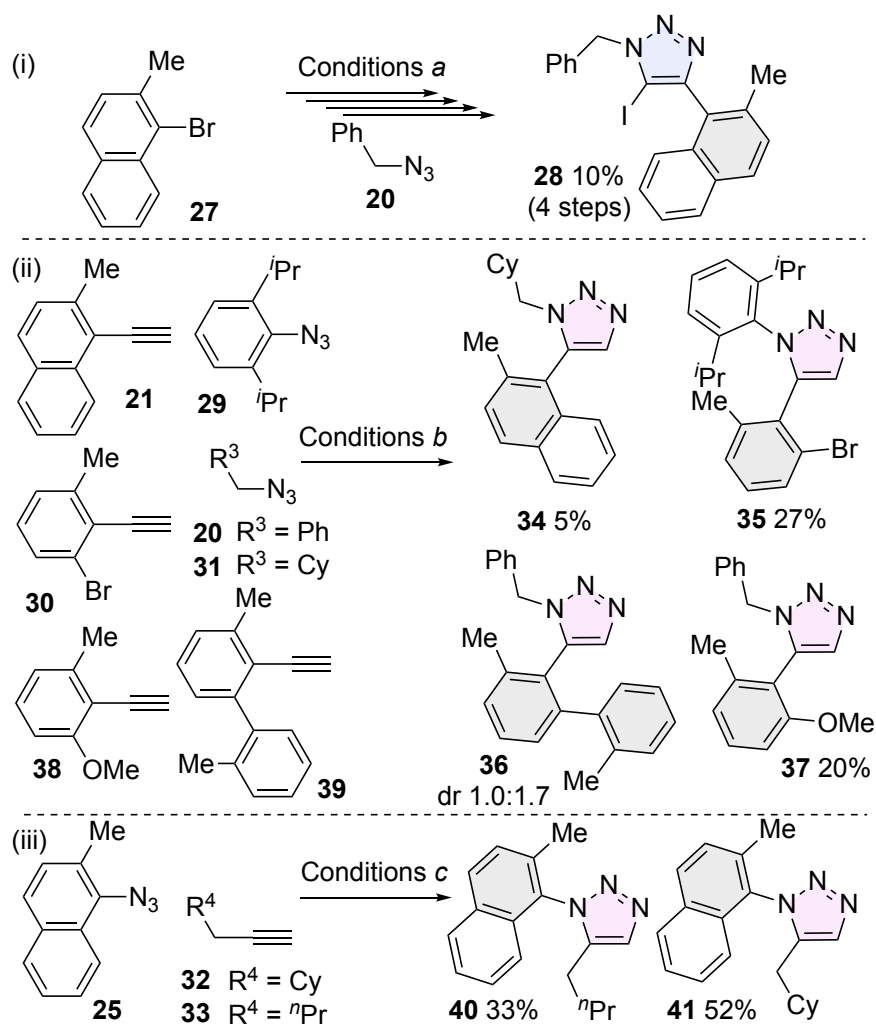
computed barriers remain somewhat higher than those determined experimentally. To address this, a number of alternative functionals were explored in order to assess whether any might be more appropriate for computing this type of barrier. Given the significant change between the minimum and the transition state in terms of steric clashing and conjugation, correctly accounting for these barriers is likely challenging and so alternative functionals are worth evaluating. The functionals listed in Table 1 were paired with the 6-31+G\*\* basis set and the IEFPCM solvation model (again with default settings for acetonitrile). Given that the experimental measurements employed temperatures of 343 K (70 °C) and 353 K (80 °C), free energies at both temperatures were computed, as well as at 298 K for comparison. These calculations revealed that all levels over-estimate the height of the barrier and that in terms of closest agreement to the two barrier heights, PBE1PBE is marginally the best but because of the good agreement in terms of absolute and relative barrier height, the B97D level of theory (entry 4) was selected as most appropriate for ranking the impact of changes in structure on rotational barrier.

**Table 1.** Free energy barrier to rotation computed with a range of functionals. These were paired with the 6-31+G\*\* basis set and IEFPCM solvation for acetonitrile. Energies are in kcal·mol<sup>-1</sup>.

Entry	Functional	Computed lowest barrier to atropisomer interconversion by triazole-aryl single bond rotation at given temperature (kcal·mol <sup>-1</sup> )					
		298 K	343 K	353 K	298 K	343 K	353 K
1	M06-2X	30.0	30.2	30.3	33.1	33.2	33.3
2	B3LYP	28.3	28.6	28.6	31.2	31.4	31.5
3	B3LYP-D3	29.5	29.7	29.7	33.0	33.2	33.3
4	B97D	27.6	<b>27.8</b> <sup>(a)</sup>	27.9	31.8	32.0	<b>32.0</b> <sup>(b)</sup>
5	M06	28.6	28.9	28.9	36.5	36.6	36.6
6	PBE1PBE	28.0	28.3	28.3	30.7	30.9	30.9

<sup>(a)</sup> Experimentally determined barrier at 343 K = 25.0 kcal·mol<sup>-1</sup>; <sup>(b)</sup> Experimentally determined barrier at 353 K = 29.0 kcal·mol<sup>-1</sup>

To probe the potential for rendering 1,4,5-tri-substituted 1,2,3-triazoles chiral by virtue of inclusion of a 5-substituent (*versus* achiral 1,4-disubstituted analogue **22**) compound **28** bearing a 5-iodosubstituent was prepared in four steps, in a 10% isolated yield (Scheme 4(i)). Analysis of the resulting proton NMR spectrum of **28** (Figure 8(i)) shows two roofed doublet signals for the benzylic methylene protons, confirming that (unlike **22**) **28** can be regarded as chiral and stable on the NMR timescale.



**Scheme 4.** (i) Synthesis of **28** under Conditions (a) bis(triphenylphosphine)palladium(II) dichloride (2 mol%), copper(I) iodide (4 mol%), triphenylphosphine (3 mol%), trimethylsilylacetylene, piperidine, reflux, then TBAF (1.0 M in THF), rt, then iodine, morpholine, toluene, rt, benzyl azide (**20**), copper(I) iodide (2 mol%), TBTA (2 mol%), THF, rt; (ii) Synthesis of **34-37** under Conditions (b) Methylmagnesium bromide (3.0 M in hexane), THF; (iii) Synthesis of **40** and **41** under Conditions (c) Diethyl zinc (1.0 M in hexane), N-methyl imidazole (20 mol%), THF.

Four 5-aryl 1,5-disubstituted 1,2,3-triazoles were prepared by a stoichiometric magnesium-mediated method (**34-37**, Scheme 4(ii)).<sup>60</sup> Compound **34** is a methylene-cyclohexyl analogue of benzyl appended **23**, which similarly to compound **23**, also displays evidence of room temperature NMR spectroscopy-detectable chirality (Figure 8(ii)), whereby the methylene protons appear as distinct signals showing geminal and vicinal coupling appearing as two roofed doublet of doublets. Compound **35** includes aryl groups at both the 1- and 5-positions of a 1,2,3-triazole core. The 5-C-substituent is a dissymmetric 2-bromo 6-methyl phenyl group whose restricted rotation confers chirality upon the molecule as determined by desymmetrisation in the proton NMR spectrum (Figure 8(iii) and (iv)) of the 2- and 6-isopropyl groups attached to the 1-N-phenyl substituent. The proton NMR spectrum of **35** features two septet signals and four doublets corresponding to the (i) CH and (ii) CH<sub>3</sub> groups of the desymmetrised isopropyl groups, respectively. Compound **36** includes a 1-N-benzyl group

alongside a 5-C-aryl group that is also doubly *ortho*-substituted, which incorporates an *ortho*-tolyl group. The presence of two aryl-bonds with the potential for restricted rotation is confirmed by proton NMR spectroscopic evidence of a 1.0:1.7 mixture of diastereoisomers (Figure 8(v)). Whilst the preference for the formation of a major diastereoisomer was intriguing this has not been stereochemically assigned or further elaborated at this stage. For compound **37**, where the 5-C-aryl fragment is a 2-methoxy-6-methyl phenyl group, clear evidence for chirality is evidenced by observation of resonances corresponding to diastereotopic benzylic protons at the 1-N-position (Figure 8(vi)).

Two 1-*N*-aryl 5-C-alkyl analogues of 5-C-benzyl-containing **26** (**40** and **41**) were prepared by a zinc-mediated method (Scheme 4(iii)).<sup>61</sup> It was not possible to observe evidence of compounds **40** and **41** being potentially chiral by restricted N-C triazole-aryl bond by proton NMR spectroscopy methods (Figure 8(vii) and (viii)). In these cases where isochronism was observed, analytical HPLC with a chiral stationary phase analysis was used which revealed two sharp peaks consistent with the presence of stable enantiomers for both compounds **40** and **41** (Figure 9(i) and (ii) respectively). Additionally, whilst compound **28** was resolved by HPLC with a chiral stationary phase, e.e. readily eroded at room temperature (see supplementary material for details).

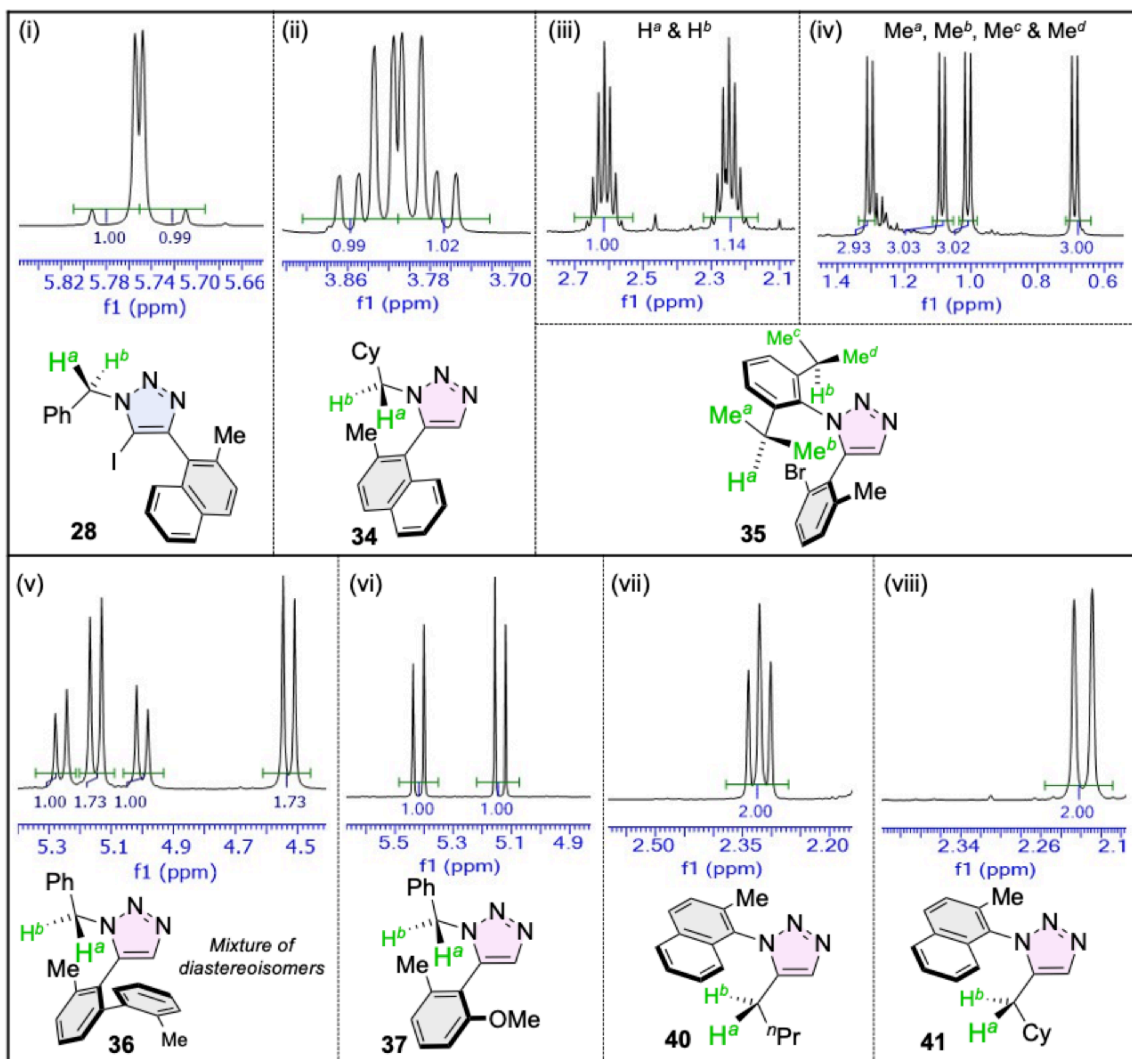


**Figure 8.** Regions of the proton NMR spectra of the compounds synthesised in Scheme 4 corresponding to potentially diagnostic environments capable of revealing a diastereotopic nature in said spectral analysis,  $\text{CDCl}_3$  298 K: (i) **28**; (ii) **34**; (iii) **35** ( $\text{CH}_2$ ); (iv) **35** (Me); (v) **36** (d.r. 1.0:1.7); (vi) **37**; (vii) **40**; (viii) **41**.

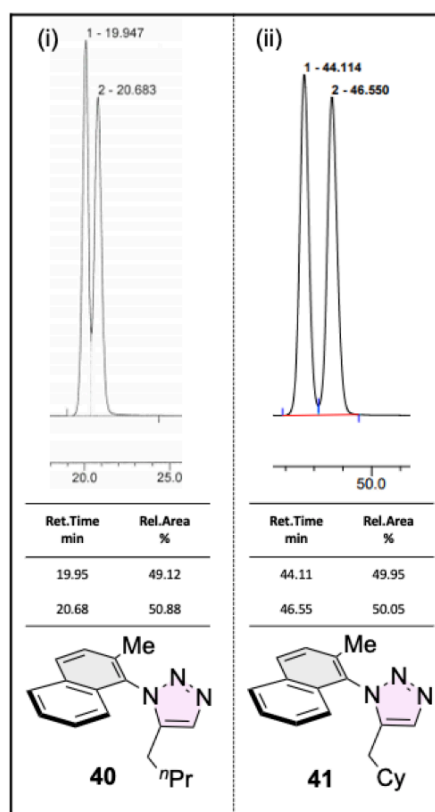


**Figure 9.** Analytical HPLC traces Phenomenex Cellulose-1, 50% acetonitrile/water, 1.0 mL/min,  $\lambda = 280$  nm (i) section of the trace from **40**; (ii) section of the trace from **41**.

Single crystals, suitable for molecular structure determination by X-ray diffraction (XRD) were obtained by slow evaporation of dichloromethane in hexane for racemates (C-C axially chiral) **23** and (N-C axially chiral) **41** (Figure 10 (i) and (ii) respectively). Both the C-linked (**23**) and N-linked (**41**) triazole-aryl motifs adopt similar orientations in the solid state and the respective methylene substituents (phenyl and cyclohexyl) are broadly presented in the same orientation. Torsion angles ascribed as  $+65.82$  ( $14$ ) $^\circ$  versus  $-96.14$  ( $13$ ) $^\circ$  respectively represent a thirty-degree deviation in real terms from one another (see supplementary material for convention defined here for ascribing sign +/- to dihedral angle). Thus, in the solid state, whether C-C or N-C axially chiral and aromatically or aliphatically substituted the conformations of these compounds are strikingly similar. Notably, and as anticipated, the C-C triazole-aryl bond of **23** is longer than the corresponding N-C triazole bond of **41** (C1-C10 =  $1.4780$  ( $15$ )  $\text{\AA}$  versus N1-C10 =  $1.4352$  ( $15$ )  $\text{\AA}$  respectively).

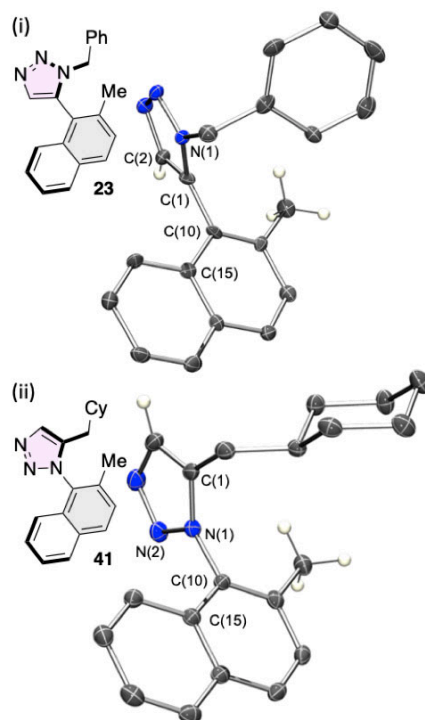


**Figure 10.** Representation of one molecule within the unit cell of the single crystal X-ray diffraction structures, most hydrogen atoms omitted for clarity, ellipsoids plot at 45% probability. Rendered in PovRay from coordinates generated in Ortep III for Windows, selected bond lengths, angles and torsions from the molecule of the unit cell depicted: (i) **23** (*rac*), C1-C10 bond length = 1.4780 (15) Å, N1-C1-C2 bond angle = +103.49 (10)° and N1-C1-C10-C15 torsion = 65.82 (14)°. Hydrogen atoms were fixed as riding models with the isotropic thermal parameters ( $U_{iso}$ ) based on the  $U_{eq}$  of the parent atom.; (ii) **41** (*rac*), N1-C10 bond length = 1.4352 (15) Å, N2-N1-C1 bond angle 111.24 (10)° and N2-N1-C10-C15 torsion = -96.14 (13)°. Methyl hydrogen atoms bonded to C20 are disordered over two positions at a refined percentage occupancy ratio of 51.8 (19) : 48.2 (19), with one set of three protons being arbitrarily depicted, and these and all other hydrogen atoms in the structure were fixed as riding models with the isotropic thermal parameters ( $U_{iso}$ ) based on the  $U_{eq}$  of the parent atom.

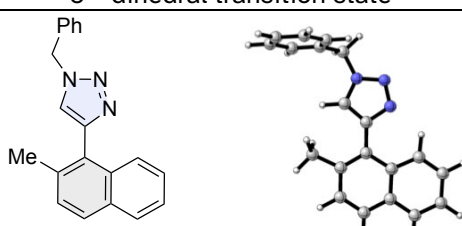
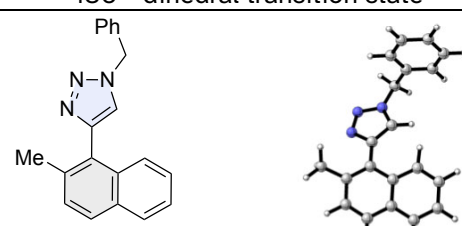
Having correlated modelling approaches to experimentally determined barriers for atropisomer interconversion (for compounds **23** and **26**) the barriers to enantiomer interconversion (racemisation) for the remaining synthesised compounds were determined using the B97D level of theory with acetonitrile solvent parameters (computed barriers to rotation at 298 K are given in Table 2, see entries 2 and 3 for compounds **23** and **26** respectively). Compound **22**, a 1,4-disubstituted triazole that would not be expected to display stable chirality, was calculated to have the lowest barrier among those determined in this study (7.1 kcal·mol<sup>-1</sup>, Table 2, entry 1). The addition of iodide at the 5-position (**28**) had already rendered the methylene protons diastereotopic by proton NMR spectroscopic analysis, and a corresponding computed barrier to rotation was found to be more than three times higher (25.3 kcal·mol<sup>-1</sup>, Table 2, entry 4). The three compounds with a methyl substituted naphthyl group at the 1-*N*-triazole position conferring axial chirality upon them with CH<sub>2</sub>-R motifs at the 5-*C*-triazole position (R = Ph (**26**), *n*-Pr (**40**) and Cy (**41**)) were calculated to have the highest barriers to enantiomer interconversion of ~32 kcal·mol<sup>-1</sup> (31.8 (Table 1), 31.9 and 32.4 kcal·mol<sup>-1</sup>

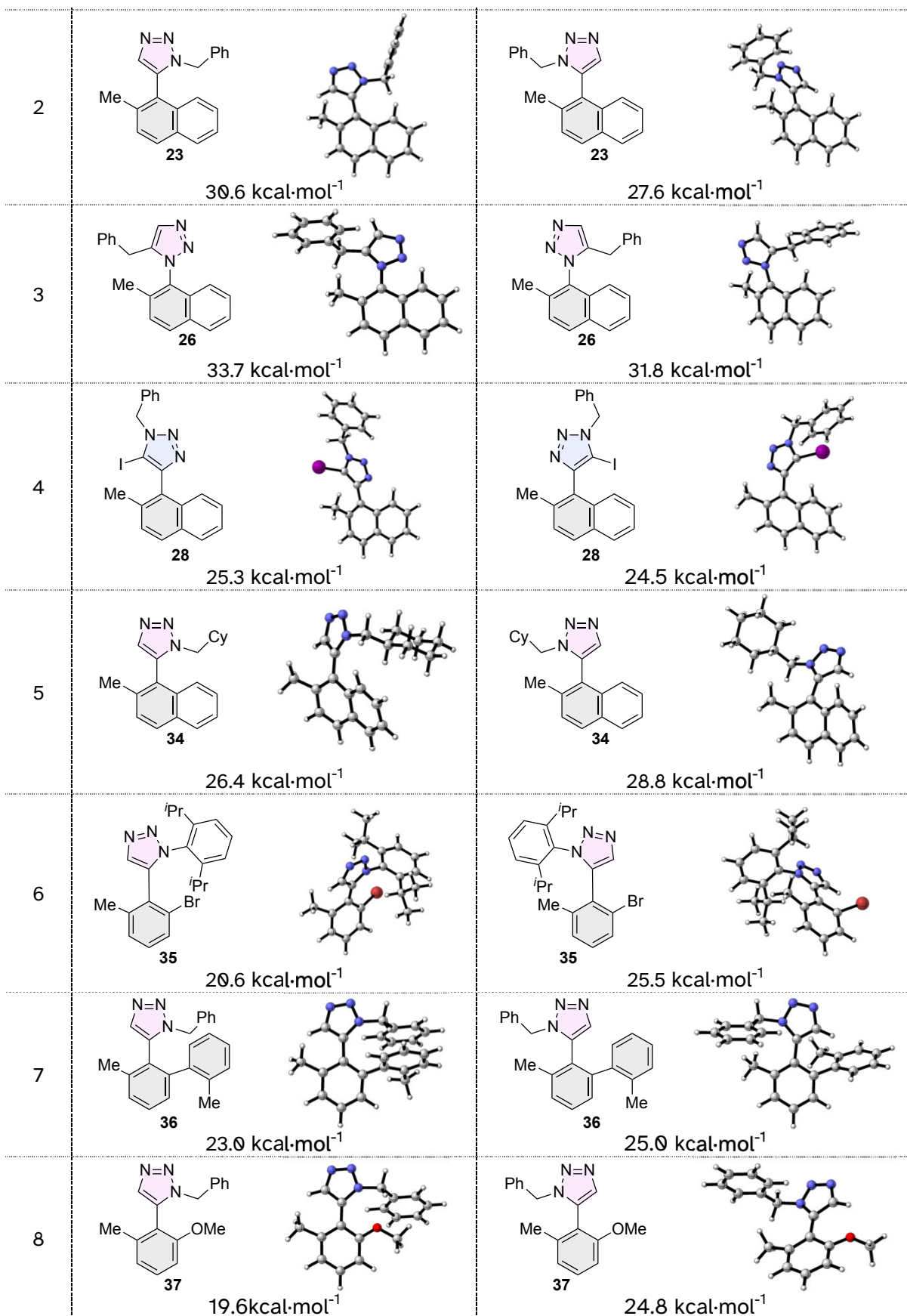
<sup>1</sup> for **26**, **40** and **41**, Table 2, entries 3, 9 and 10 respectively). Compound **23** and its cyclohexyl-containing congener **34** were computed to have lower, albeit similar, barriers to enantiomer interconversion (27.6 (Table 1) and 26.4 kcal·mol<sup>-1</sup>, Table 2, entries 2 and 5 respectively). Triazoles with chirality-conferring dissymmetric 2,6-disubstituted phenyl groups at the 5-C-triazole position (**35-37**) were calculated to have somewhat lower barriers to enantiomer interconversion (20.6, 23.0 and 19.6 kcal·mol<sup>-1</sup>, Table 2, entries 6, 7 and 8 respectively). Given barriers to epimerisation, and thus enantiomer stability, are greater for C-N rotation-restricted triazoles over C-C rotation restricted triazoles, nitrogen's lone pair in the 2-position, as well as N-C versus C-C bond length, may contribute to the observed trends in enantiomer stability.<sup>93</sup>

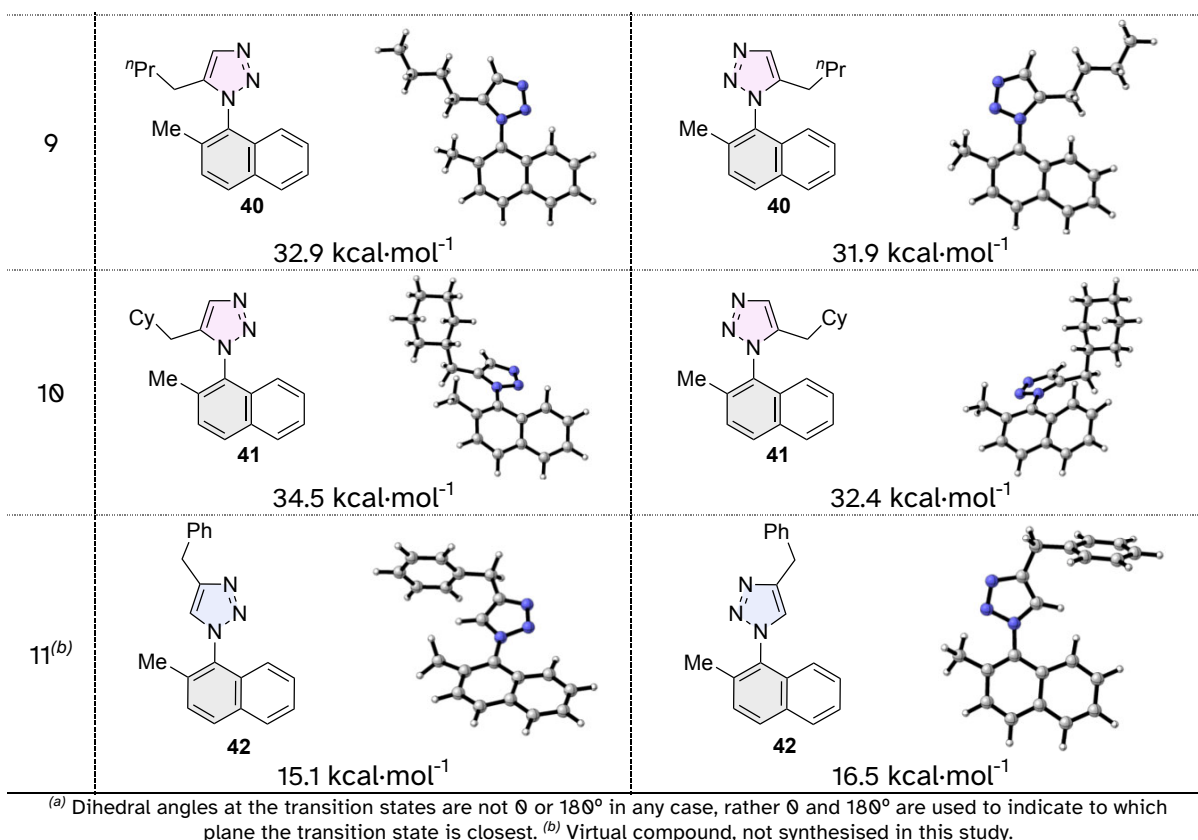
94

Upon visual inspection of the computed two lowest barriers to enantiomer interconversions it can be observed that 1,4-disubstituted triazoles (Table 2, entries 1 and 11, compounds **22** and **42** with a triazole-aryl C-C and N-C bond respectively) have a lower barrier with the CH proton of the triazole presented towards the methyl group of the aryl fragment. Compound 28 (Table 2, entry 4), is the 5-iodo analogue of compound **22**, wherein the energy lower transition state arises from an orientation with iodine pointing away from the methyl substituent of the aryl fragment. Whilst the barrier is too low to lead to observable chirality at room temperature, the overall structural shape of the transition state for interconversion has substituents in approximately equivalent positions. The 1,5-disubstituted triazoles with N-C triazole-aryl bond restriction leading to chirality (Table 2, entries 3, 9 and 10, compounds **26**, **40** and **41** respectively) have a lower barrier where the triazoles 2-N nitrogen is presented towards the 2-methyl substituent of the aryl fragment. In all but the case of compound **23** (Table 2, entry 2) C-C triazole-aryl 1,5-disubstituted triazoles show a similar motif for the lowest barrier to enantiomer interconversion, namely the CH proton of the triazole is presented towards the methyl group of the aryl fragment.

**Table 2.** Computed barriers to atropisomer interconversion (kcal·mol<sup>-1</sup>) by triazole-aryl single bond rotation at 298 K, in acetonitrile, using the B97D level of theory for compounds **22**, **23**, **26**, **28**, **34-37**, **40-42**. See supplementary material for coordinates and ground states.

Entry	~0° dihedral transition state <sup>(a)</sup>	~180° dihedral transition state <sup>(a)</sup>
1	 <p><b>22</b> 7.1 kcal·mol<sup>-1</sup></p>	 <p><b>22</b> 9.6 kcal·mol<sup>-1</sup></p>





To computationally elaborate upon the N-C *versus* C-C triazole-aryl rotational barrier, the barrier to rotation of 1,4-substituted 1,2,3-triazole **42** was investigated. Compound **42** is an analogue of the synthesised 1,4-disubstituted **22** wherein the benzyl and naphthyl motifs are swapped (Table 2, entry 11). The computed barrier to rotation for the *N*-aryl **42** was twice as high as that for the *C*-aryl isomer **22** (15.1 *versus* 7.1 kcal·mol<sup>-1</sup>), which is consistent with aforementioned observations of greater barriers to rotation for *N*-aryl substituted triazoles.

## Conclusion

Ten 1,2,3-triazoles were synthesised to investigate features pertaining to the potential for such triazoles to be (usefully) axially chiral. The measured and computed barriers to enantiomer interconversion along with solid state measurements (Figure 10) are consistent with the propensity for C<sub>sp2</sub>-N<sub>sp2</sub> bond lengths to typically be shorter than C<sub>sp2</sub>-C<sub>sp2</sub> bonds,<sup>95</sup> consequently providing a greater steric barrier to rotation in the *N*-aryl axially chiral systems. This appears to dominate over other parameters that might lead to increasing or decreasing the barrier to enantiomer interconversion, suggesting the best candidates for further exploration of stable triazole axial chirality to be 1-aryl 5- (at least) di-substituted 1,2,3-triazoles. Whilst the barriers to racemisation of these compounds do not yet challenge the stability of biaryls like BINOL (barrier of 37-38 kcal·mol<sup>-1</sup>),<sup>96, 97</sup> the intermediate/hemi stability

may be of use in transient or switchable state arenas and offers a platform from which to develop ever more robust and applicable chemistries upon the triazole stage.

### **Supplementary material**

A file containing synthetic procedures and experimental data thereof, spectrums and chromatograms, XRD data and computational coordinates is available. The supplementary material file includes additional references cited therein.<sup>98-116</sup> Summaries of crystal structure data are included, and full datasets may be accessed at CCDC deposit numbers CCDC 2111317 (**23**) and CCDC 2111318 (**41**).

### **Acknowledgements**

The authors are grateful to the University of Birmingham for support including PhD studentships to FM and WDGB. Dr Christopher Williams and Dr Chi Tsang are thanked for the helpful discussions about mass spectrometry. JSF, WDGB and BRB acknowledge the support of a Wellcome Trust ISSF award within the University of Birmingham and a Royal Society Research Grant (2012/R1) that underpinned aspects of this work. WDGB would also like to thank the Royal Society of Chemistry, Society for Chemical Industry and the School of Chemistry at the University. Facilities at the University of Birmingham used to obtain analytical data were supported by the EPSRC (EP/K039245/1). AGL acknowledges the assistance given by Research IT and the use of the Computational Shared Facility at The University of Manchester.

### **Corresponding Author**

\*Corresponding authors: JSF [j.s.fossey@bham.ac.uk](mailto:j.s.fossey@bham.ac.uk) (molecular synthesis and analysis), BRB [b.r.buckley@lboro.ac.uk](mailto:b.r.buckley@lboro.ac.uk) (heterocyclic chemistry) or AGL [andrew.leach@manchester.ac.uk](mailto:andrew.leach@manchester.ac.uk) (computational aspects).

### **Author Contributions**

FM conducted the majority of the chemical synthesis, contributed to critical decisions and wrote sections of the manuscript; WDGB conducted preliminary experiments and synthesised **28**; LM collected, analysed and solved the XRD structures of this report; CSLD contributed to NMR spectroscopic experiments; BRB co-conceived the study and contributed to aspects of project supervision; AGL conducted all computational experiments, interpreted those results and wrote aspects of the manuscript; JSF co-conceived the study and experiments, supervised the project, made critical decisions and wrote the manuscript. All co-authors analysed data, contributed ideas and commented on the manuscript.

## Competing financial interests

The authors declare no competing financial interests.

## References

- 1 Moss, G. P. *Pure Appl. Chem.* **1996**, *68*, 2193.
- 2 Cross, L. C.; Klyne, W. *Pure Appl. Chem.* **1976**, *45*, 11.
- 3 Alkorta, I.; Elguero, J.; Roussel, C.; Vanthuynne, N.; Piras, P. In *Chapter 1 - Atropisomerism and Axial Chirality in Heteroaromatic Compounds*; Academic Press, 2012; Vol. 105. pp 1.
- 4 Kuhn, R. In *Molekulare Asymmetrie*; Franz-Deutike, Leipzig-Wien, 1933, 803–824.
- 5 Bringmann, G.; Price Mortimer, A. J.; Keller, P. A.; Gresser, M. J.; Garner, J.; Breuning, M. *Angew. Chem. Int. Ed.* **2005**, *44*, 5384.
- 6 Ōki, M. In *Recent Advances in Atropisomerism*; John Wiley & Sons, 1983. pp 1.
- 7 Smyth, J. E.; Butler, N. M.; Keller, P. A. *Nat. Prod. Rep.* **2015**, *32*, 1562.
- 8 Hughes, C. C.; Yang, Y.-L.; Liu, W.-T.; Dorrestein, P. C.; Clair, J. J. L.; Fenical, W. *J. Am. Chem. Soc.* **2009**, *131*, 12094.
- 9 Kovacic, P. *Curr. Med. Chem.* **2003**, *10*, 2711.
- 10 Liu, Y.; Kurtan, T.; Yun Wang, C.; Han Lin, W.; Orfali, R.; Muller, W. E.; Daletos, G.; Proksch, P. *J. Antibiot. (Tokyo)* **2016**, *69*, 702.
- 11 Boyer, F.-D.; Hanna, I. *Org. Lett.* **2007**, *9*, 715.
- 12 Xing, L.; Mathias, J. In *Medicinal Chemistry Case History: Structure-Based Drug Design of Oral and Inhaled p38 MAP Kinase Inhibitors as Clinical Candidates*; Elsevier, Oxford, 2017. pp 408.
- 13 Toenjes, S. T.; Gustafson, J. L. *Future Med. Chem.* **2018**, *10*, 409.
- 14 Beutner, G.; Carrasquillo, R.; Geng, P.; Hsiao, Y.; Huang, E. C.; Janey, J.; Katipally, K.; Kolotuchin, S.; La Porte, T.; Lee, A.; Lobben, P.; Lora-Gonzalez, F.; Mack, B.; Mudryk, B.; Qiu, Y.; Qian, X.; Ramirez, A.; Razler, T. M.; Rosner, T.; Shi, Z.; Simmons, E.; Stevens, J.; Wang, J.; Wei, C.; Wisniewski, S. R.; Zhu, Y. *Org. Lett.* **2018**, *20*, 3736.
- 15 Glunz, P. W. *Bioorg. Med. Chem. Lett.* **2018**, *28*, 53.
- 16 Clayden, J.; Moran, W. J.; Edwards, P. J.; LaPlante, S. R. *Angew. Chem. Int. Ed.* **2009**, *48*, 6398.
- 17 Parmar, D.; Sugiono, E.; Raja, S.; Rueping, M. *Chem. Rev.* **2014**, *114*, 9047.
- 18 Hashimoto, T.; Sakata, K.; Tamakuni, F.; Dutton, M. J.; Maruoka, K. *Nat. Chem.* **2013**, *5*, 240.
- 19 Shirakawa, S.; Maruoka, K. *Angew. Chem. Int. Ed.* **2013**, *52*, 4312.
- 20 Brunel, J. M. *Chem. Rev.* **2005**, *105*, 857.
- 21 Kumarasamy, E.; Raghunathan, R.; Sibi, M. P.; Sivaguru, J. *Chem. Rev.* **2015**, *115*, 11239.
- 22 Noyori, R.; Takaya, H. *Acc. Chem. Res.* **1990**, *23*, 345.
- 23 Rokade, B. V.; Guiry, P. J. *ACS Catal.* **2018**, *8*, 624.
- 24 Cardoso, F. S. P.; Abboud, K. A.; Aponick, A. *J. Am. Chem. Soc.* **2013**, *135*, 14548.
- 25 Mishra, S.; Liu, J.; Aponick, A. *J. Am. Chem. Soc.* **2017**, *139*, 3352.

- 26 Bonne, D.; Rodriguez, J. *Eur. J. Org. Chem.* **2018**, 2018, 2417.
- 27 Wang, F.; Li, S.; Qu, M.; Zhao, M.-X.; Liu, L.-J.; Shi, M. *Chem. Commun.* **2011**, 47, 12813.
- 28 Pappoppula, M.; Cardoso, F. S. P.; Garrett, B. O.; Aponick, A. *Angew. Chem. Int. Ed.* **2015**, 54, 15202.
- 29 Paioti, P. H. S.; Abboud, K. A.; Aponick, A. *J. Am. Chem. Soc.* **2016**, 138, 2150.
- 30 Etayo, P.; Escudero-Adán, E. C.; Pericàs, M. A. *Cat. Sci. Tech.* **2017**, 7, 4830.
- 31 DeRatt, L. G.; Pappoppula, M.; Aponick, A. *Angew. Chem. Int. Ed.* **2019**, 58, 8416.
- 32 Rokade, B. V.; Guiry, P. J. *ACS Catal.* **2017**, 7, 2334.
- 33 Foyle, É. M.; White, N. G. *Chem.-Asian J.* **2021**, 16, 575.
- 34 Schulze, B.; Schubert, U. S. *Chem. Soc. Rev.* **2014**, 43, 2522.
- 35 Suntrup, L.; Kleoff, M.; Sarkar, B. *Dalton Trans.* **2018**, 47, 7992.
- 36 Byrne, J. P.; Kitchen, J. A.; Gunnlaugsson, T. *Chem. Soc. Rev.* **2014**, 43, 5302.
- 37 McCarney, E. P.; Hawes, C. S.; Blasco, S.; Gunnlaugsson, T. *Dalton Trans.* **2016**, 45, 10209.
- 38 Dheer, D.; Singh, V.; Shankar, R. *Bioorg. Chem.* **2017**, 71, 30.
- 39 Song, H.; Rogers, N. J.; Brabec, V.; Clarkson, G. J.; Coverdale, J. P. C.; Kostrhunova, H.; Phillips, R. M.; Postings, M.; Shepherd, S. L.; Scott, P. *Chem. Commun.* **2020**, 56, 6392.
- 40 Adarsh, S.; Preeti, S.; Ramkishore, A. *Curr. Chem. Biol.* **2020**, 14, 71.
- 41 Lau, Y. H.; Rutledge, P. J.; Watkinson, M.; Todd, M. H. *Chem. Soc. Rev.* **2011**, 40, 2848.
- 42 Shaily, Kumar, A.; Parveen, I.; Ahmed, N. *Luminescence* **2018**, 33, 713.
- 43 Huang, W.; Zhang, Y.-C.; Jin, R.; Chen, B.-L.; Chen, Z. *Organometallics* **2018**, 37, 3196.
- 44 Zurro, M.; Mancheño, O. G. *Chem. Rec.* **2017**, 17, 485.
- 45 Schweinfurth, D.; Hettmanczyk, L.; Suntrup, L.; Sarkar, B. *Z. Anorg. Allg. Chem.* **2017**, 643, 554.
- 46 Liu, E.-C.; Topczewski, J. J. *J. Am. Chem. Soc.* **2021**, 143, 5308.
- 47 Alexander, J. R.; Ott, A. A.; Liu, E.-C.; Topczewski, J. J. *Org. Lett.* **2019**, 21, 4355.
- 48 Liao, K.; Gong, Y.; Zhu, R.-Y.; Wang, C.; Zhou, F.; Zhou, J. *Angew. Chem. Int. Ed.* **2021**, 60, 8488.
- 49 Liu, E.-C.; Topczewski, J. J. *J. Am. Chem. Soc.* **2019**, 141, 5135.
- 50 Zhou, F.; Tan, C.; Tang, J.; Zhang, Y.-Y.; Gao, W.-M.; Wu, H.-H.; Yu, Y.-H.; Zhou, J. *J. Am. Chem. Soc.* **2013**, 135, 10994.
- 51 Xi, W.; Scott, T. F.; Kloxin, C. J.; Bowman, C. N. *Adv. Funct. Mater.* **2014**, 24, 2572.
- 52 Arslan, M.; Acik, G.; Tasdelen, M. A. *Polym. Chem.* **2019**, 10, 3806.
- 53 Ahmad Fuaad, A. A. H.; Azmi, F.; Skwarczynski, M.; Toth, I. *Molecules* **2013**, 18.
- 54 Huisgen, R. *Pure Appl. Chem.* **1989**, 61, 613.
- 55 Huisgen, R.; Szeimies, G.; Möbius, L. *Chem. Ber.* **1967**, 100, 2494.
- 56 Rostovtsev, V. V.; Green, L. G.; Fokin, V. V.; Sharpless, K. B. *Angew. Chem. Int. Ed.* **2002**, 41, 2596.
- 57 Tornøe, C. W.; Christensen, C.; Meldal, M. *J. Org. Chem.* **2002**, 67, 3057.

- 58 Kolb, H. C.; Finn, M. G.; Sharpless, K. B. *Angew. Chem. Int. Ed.* **2001**, *40*, 2004.
- 59 Meldal, M.; Tornøe, C. W. *Chem. Rev.* **2008**, *108*, 2952.
- 60 Krasinski, A.; Fokin, V. V.; Sharpless, K. B. *Org. Lett.* **2004**, *6*, 1237.
- 61 Smith, C. D.; Greaney, M. F. *Org. Lett.* **2013**, *15*, 4826.
- 62 Johansson, J. R.; Beke-Somfai, T.; Said Stålsmeden, A.; Kann, N. *Chem. Rev.* **2016**, *116*, 14726.
- 63 Farooq, T.; Sydnese, L. K.; Törnroos, K. W.; Haug, B. E. *Synthesis* **2012**, *44*, 2070.
- 64 Zhang, L.; Chen, X.; Xue, P.; Sun, H. H. Y.; Williams, I. D.; Sharpless, K. B.; Fokin, V. V.; Jia, G. *J. Am. Chem. Soc.* **2005**, *127*, 15998.
- 65 Kim, W. G.; Kang, M. E.; Lee, J. B.; Jeon, M. H.; Lee, S.; Lee, J.; Choi, B.; Cal, P. M. S. D.; Kang, S.; Kee, J.-M.; Bernardes, G. J. L.; Rohde, J.-U.; Choe, W.; Hong, S. Y. *J. Am. Chem. Soc.* **2017**.
- 66 Nguyen, Q.-H.; Guo, S.-M.; Royal, T.; Baudoin, O.; Cramer, N. *J. Am. Chem. Soc.* **2020**, *142*, 2161.
- 67 Vroemans, R.; Ribone, S. R.; Thomas, J.; Van Meervelt, L.; Ollevier, T.; Dehaen, W. *Org. Biomol. Chem.* **2021**, *19*, 6521.
- 68 Laborde, C.; Wei, M.-M.; van der Lee, A.; Deydier, E.; Daran, J.-C.; Volle, J.-N.; Poli, R.; Pirat, J.-L.; Manoury, E.; Virieux, D. *Dalton Trans.* **2015**, *44*, 12539.
- 69 Sevrain, N.; Volle, J.-N.; Pirat, J.-L.; Ayad, T.; Virieux, D. *RSC Adv.* **2017**, *7*, 52101.
- 70 Sevrain, N.; Volle, J.-N.; Pirat, J.-L.; Ayad, T.; Virieux, D. *Eur. J. Org. Chem.* **2018**, *2018*, 2267.
- 71 Brittain, W. D. G.; Buckley, B. R.; Fossey, J. S. *Chem. Commun.* **2015**, *51*, 17217.
- 72 Zhai, W.; Chapin, B. M.; Yoshizawa, A.; Wang, H.-C.; Hodge, S. A.; James, T. D.; Anslyn, E. V.; Fossey, J. S. *Org. Chem. Front.* **2016**, *3*, 918.
- 73 Brittain, W. D. G.; Chapin, B. M.; Zhai, W.; Lynch, V. M.; Buckley, B. R.; Anslyn, E. V.; Fossey, J. S. *Org. Biomol. Chem.* **2016**, *14*, 10778.
- 74 Zhai, W.; Male, L.; Fossey, J. S. *Chem. Commun.* **2017**, *53*, 2218.
- 75 Zhao, Y.; Wakeling, M. G.; Meloni, F.; Sum, T. J.; van Nguyen, H.; Buckley, B. R.; Davies, P. W.; Fossey, J. S. *Eur. J. Org. Chem.* **2019**, *2019*, 5540.
- 76 Zhao, Y.; van Nguyen, H.; Male, L.; Craven, P.; Buckley, B. R.; Fossey, J. S. *Organometallics* **2018**, *37*, 4224.
- 77 Brittain, W. D. G.; Buckley, B. R.; Fossey, J. S. *Chem. Commun.* **2015**, *51*, 17217.
- 78 Brittain, W. D. G.; Buckley, B. R.; Fossey, J. S. *ACS Catal.* **2016**, *6*, 3629.
- 79 Brittain, W. D. G.; Dalling, A. G.; Sun, Z.; Duff, C. S. L.; Male, L.; Buckley, B. R.; Fossey, J. S. *Sci. Rep.* **2019**, *9*, 15086.
- 80 Feula, A.; Male, L.; Fossey, J. S. *Org. Lett.* **2010**, *12*, 5044.
- 81 Hadzhiev, Y.; Qureshi, H. K.; Wheatley, L.; Cooper, L.; Jasiulewicz, A.; Van Nguyen, H.; Wragg, J. W.; Poovathumkadavil, D.; Conic, S.; Bajan, S.; Sik, A.; Hutvågner, G.; Tora, L.; Gambus, A.; Fossey, J. S.; Müller, F. *Nat. Commun.* **2019**, *10*, 691.
- 82 Mahadari, M. K.; Tague, A. J.; Keller, P. A.; Pyne, S. G. *Tetrahedron* **2020**, 131916.
- 83 Bryant, R. G. *J. Chem. Educ.* **1983**, *60*, 933.
- 84 Sepsey, A.; Németh, D. R.; Németh, G.; Felinger, A. *J. Chromatogr. A* **2018**, *1564*, 155.
- 85 Stewart, W. E.; Siddall, T. H. *Chem. Rev.* **1970**, *70*, 517.
- 86 LaPlante, S. R.; Edwards, P. J.; Fader, L. D.; Jakalian, A.; Hucke, O. *ChemMedChem* **2011**, *6*, 505.

- 87 Zhao, Y.; Truhlar, D. G. *Theor. Chem. Acc.* **2008**, *120*, 215.
- 88 Zhao, Y.; Truhlar, D. G. *Acc. Chem. Res.* **2008**, *41*, 157.
- 89 Tomasi, J.; Mennucci, B.; Cammi, R. *Chem. Rev.* **2005**, *105*, 2999.
- 90 Frisch, M. J.; Trucks, G. W.; Schlegel, H. B.; Scuseria, G. E.; Robb, M. A.; Cheeseman, J. R.; Scalmani, G.; Barone, V.; Petersson, G. A.; Nakatsuji, H.; Li, X.; Caricato, M.; Marenich, A. V.; Bloino, J.; Janesko, B. G.; Gomperts, R.; Mennucci, B.; Hratchian, H. P.; Ortiz, J. V.; Izmaylov, A. F.; Sonnenberg, J. L.; Williams, Ding, F.; Lipparini, F.; Egidi, F.; Goings, J.; Peng, B.; Petrone, A.; Henderson, T.; Ranasinghe, D.; Zakrzewski, V. G.; Gao, J.; Rega, N.; Zheng, G.; Liang, W.; Hada, M.; Ehara, M.; Toyota, K.; Fukuda, R.; Hasegawa, J.; Ishida, M.; Nakajima, T.; Honda, Y.; Kitao, O.; Nakai, H.; Vreven, T.; Throssell, K.; Montgomery Jr., J. A.; Peralta, J. E.; Ogliaro, F.; Bearpark, M. J.; Heyd, J. J.; Brothers, E. N.; Kudin, K. N.; Staroverov, V. N.; Keith, T. A.; Kobayashi, R.; Normand, J.; Raghavachari, K.; Rendell, A. P.; Burant, J. C.; Iyengar, S. S.; Tomasi, J.; Cossi, M.; Millam, J. M.; Klene, M.; Adamo, C.; Cammi, R.; Ochterski, J. W.; Martin, R. L.; Morokuma, K.; Farkas, O.; Foresman, J. B.; Fox, D. J. *Gaussian 09 Revision A.02* **2016**, Wallingford.
- 91 The sign (+/-) of the given dihedral angles and the defined zero (versus 180) degrees notation used is systematically described in the supporting information to this manuscript.
- 92 Luchini, G.; Alegre-Requena, J. V.; Funes-Ardoiz, I.; Paton, R. S. *F1000Research* **2020**, *9* (*Chem Inf Sci*), 291.
- 93 Allinger, N. L.; Hirsch, J. A.; Miller, M. A. *Tetrahedron Lett.* **1967**, *8*, 3729.
- 94 Robb, M. A.; Haines, W. J.; Csizmadia, I. G. *J. Am. Chem. Soc.* **1973**, *95*, 42.
- 95 Allen, F. H.; Kennard, O.; Watson, D. G.; Brammer, L.; Orpen, A. G.; Taylor, R. *J. Chem. Soc., Perk. Trans. 2* **1987**, S1.
- 96 Patel, D. C.; Woods, R. M.; Breitbach, Z. S.; Berthod, A.; Armstrong, D. W. *Tetrahedron Asymmetr.* **2017**, *28*, 1557.
- 97 Meca, L.; Řeha, D.; Havlas, Z. *J. Org. Chem.* **2003**, *68*, 5677.
- 98 Aliprantis, A. O.; Canary, J. W. *J. Am. Chem. Soc.* **1994**, *116*, 6985.
- 99 Alvarez, S. G.; Alvarez, M. T. *Synthesis* **1997**, *1997*, 413.
- 100 Anneser, M. R.; Elpitiya, G. R.; Townsend, J.; Johnson, E. J.; Powers, X. B.; DeJesus, J. F.; Vogiatzis, K. D.; Jenkins, D. M. *Angew. Chem. Int. Ed.* **2019**, *58*, 8115.
- 101 Cong, X.; Tang, H.; Zeng, X. *J. Am. Chem. Soc.* **2015**, *137*, 14367.
- 102 Dolomanov, O. V.; Bourhis, L. J.; Gildea, R. J.; Howard, J. A. K.; Puschmann, H. *J. Appl. Crystallogr.* **2009**, *42*, 339.
- 103 Frisch, M. J.; Trucks, G. W.; Schlegel, H. B.; Scuseria, G. E.; Robb, M. A.; Cheeseman, J. R.; Scalmani, G.; Barone, V.; Mennucci, B.; Petersson, G. A.; Nakatsuji, H.; Li, X.; Caricato, M.; Hratchian, H. P.; Izmaylov, A. F.; Bloino, J.; Zheng, G.; Sonnenberg, J. L.; Hada, M.; Ehara, M.; Toyota, K.; Fukuda, R.; Hasegawa, J.; Ishida, M.; Nakajima, T.; Honda, Y.; Kitao, O.; Nakai, H.; Vreven, T.; Montgomery Jr., J. A.; Peralta, J. E.; Ogliaro, F.; Bearpark, M.; Heyd, J. J.; Brothers, E.; Kudin, K. N.; Staroverov, V. N.; Keith, T.; Kobayashi, R.; Normand, J.; Raghavachari, K.; Rendell, A.; Burant, J. C.; Iyengar, S. S.; Tomasi, J.; Cossi, M.; Rega, N.; Millam, J. M.; Klene, M.; Knox, J. E.; Cross, J. B.; Bakken, V.; Adamo, C.; Jaramillo, J.; Gomperts, R.; Stratmann, R. E.; Yazyev, O.; Austin, A. J.; Cammi, R.; Pomelli, C.; Ochterski, J. W.; Martin, R. L.; Morokuma, K.; Zakrzewski, V. G.; Voth, G. A.; Salvador, P.; Dannenberg, J. J.; Dapprich, S.; Daniels, A. D.; Farkas, O.; Foresman, J. B.; Ortiz, J. V.; Cioslowski, J.; Fox, D. J. *Gaussian 09, Revision D.01 Gaussian, Inc., Wallingford CT, 2013*.
- 104 Gallant, P.; D'Haenens, L.; Vandewalle, M. *Synth. Commun.* **1984**, *14*, 155.
- 105 Hehre, W. J.; Ditchfield, R.; Pople, J. A. *The Journal of Chemical Physics* **1972**, *56*, 2257.
- 106 Jančařík, A.; Rybáček, J.; Cocq, K.; Vacek Chocholoušová, J.; Vacek, J.; Pohl, R.; Bednářová, L.; Fiedler, P.; Císařová, I.; Stará, I. G.; Starý, I. *Angew. Chem. Int. Ed.* **2013**, *52*, 9970.
- 107 Kadoya, N.; Murai, M.; Ishiguro, M.; Uenishi, J. i.; Uemura, M. *Tetrahedron Lett.* **2013**, *54*, 512.
- 108 Le, C. M.; Menzies, P. J. C.; Petrone, D. A.; Lautens, M. *Angew. Chem. Int. Ed.* **2015**, *54*, 254.
- 109 Lin, H.; Truhlar, D. G. *Theor. Chem. Acc.* **2006**, *117*, 185.
- 110 Mennucci, B.; Cancès, E.; Tomasi, J. *J. Phys. Chem. B* **1997**, *101*, 10506.

- 111 Mitchell, G.; Rees, C. W. *J. Chem. Soc., Perkin Trans. 1* **1987**, 403.
- 112 Quesada, E.; Raw, S. A.; Reid, M.; Roman, E.; Taylor, R. J. K. *Tetrahedron* **2006**, 62, 6673.
- 113 Sheldrick, G. *Acta Crystallogr. Sect. A* **2015**, 71, 3.
- 114 Sheldrick, G. *Acta Crystallogr. Sect. C* **2015**, 71, 3.
- 115 Suzuki, T.; Ota, Y.; Kasuya, Y.; Mutsuga, M.; Kawamura, Y.; Tsumoto, H.; Nakagawa, H.; Finn, M. G.; Miyata, N. *Angew. Chem. Int. Ed.* **2010**, 49, 6817.
- 116 Yong, Q.; Sun, B.; Zhang, F.-L. *Tetrahedron Lett.* **2019**, 60, 151263.